Magnetic Coupling Constants and Spin Density Maps for Heterobinuclear Complexes $GdCu(OTf)_3(bdmap)_2(H_2O)\cdot THF$, $[Gd(C_4H_7ON)_4(H_2O)_3][Fe(CN)_6]\cdot 2H_2O$, and $[Gd(C_4H_7ON)_4(H_2O)_3][Cr(CN)_6]\cdot 2H_2O$: A Density Functional Study

Feng Yan and Zhida Chen*

State Key Laboratory of Rare Earth Materials Chemistry and Applications, Department of Chemistry, Peking University, Beijing 100871, China, and Peking University−The University of Hong Kong Joint Laboratory in Rare Earth Materials and Bioinorganic Chemistry, Beijing 100871, China

Received: November 17, 1999; In Final Form: March 16, 2000

Magnetic coupling constants *J* for the complete structures of heterobinuclear compounds $GdCu(OTf)_3(bdmap)_2(H_2O)\cdot THF$ (**1**, $Gd^{III}Cu^{II}$), $[Gd(C_4H_7ON)_4(H_2O)_3][Fe(CN)_6]\cdot 2H_2O$ (**2**, $Gd^{III}Fe^{III}$), and $[Gd(C_4H_7ON)_4(H_2O)_3][Cr(CN)_6]\cdot 2H_2O$ (**3**, $Gd^{III}Cr^{III}$) have been calculated by the combination of the broken-symmetry approach with the spin project method under the DFT framework. The calculated *J* values (3.6 (**1**), 8.1 (**2**), and 20.3 cm^{-1} (**3**)) conform well to that of experimental findings (2.9(2) (**1**), 0.74(3) (**2**), and 0.40(2) cm^{-1} (**3**)) with a small difference in absolute value. The compounds **1**−**3**, whose *J* values are all positive, show ferromagnetic couplings between two metal centers; thus, their ground states are all in high-spin states. The spin density distributions are discussed in detail on the basis of Mulliken population analysis, taking into account the coexistence of spin delocalization and spin polarization mechanisms. For **1**, the spin distribution in the ground state may be understood as a result of the competition between two mechanisms: a spin delocalization from Cu(II) and a spin polarization of Gd^{III}, and the former is dominant. In the cases of **2** and **3**, both transition metal (Fe^{III} or Cr^{III}) and rare earth Gd^{III} display a spin polarization effect on the surrounding atoms, where a counteraction of the opposite polarization effects leads a low spin density on the bridging ligand C1N1. In the ground state of **3**, the stronger polarization effect of Cr(III) even causes the positive spin density on the adjacent bridging atom N1, different from the situation in **2**.

Introduction

The magnetic properties of binuclear transition metal complexes have received much attention among computational chemists, due mainly to being a starting point of studies on magneto−structural correlations. The typical transition metal complexes studied theoretically are hydroxo-, alkoxo-,[1] and azido-bridged[2,3] Cu^{II} binuclear species. Meanwhile, the increasingly improved experimental techniques may give us more information of the magnetic coupling mechanism. Kahn et al. have recently measured the polarized neutron diffraction (PND) data for oxamido-bridged $Mn^{II}Cu^{II}$ [4] and azido-bridged Cu^{II} binuclear[5] compounds and determined the distributions of their spin densities. Up till now, the research on this field was mainly concentrated on binuclear systems of transition metals, i.e., 3d−3d systems. However, a great diversity of situations may be encountered if the interaction is between two different magnetic centers, namely in heterobinuclear compounds. Furthermore, due to the important role of rare earth elements in magnetic materials, the rare earth (RE)−transition metal (M) compounds are of concern widely. Some complexes of this kind, including $Cu^{II}Gd^{III}$ and $Cu^{II}Yb^{III}$, etc., have been synthesized experimentally.[6] For the sake of calculation, some typical RE−M complexes have been synthesized and characterized in our laboratory. In this paper, we select three complexes in order to extend the research of magnetic coupling mechanism to the RE−M system, i.e., 4f−3d system, which are the following: $GdCu(OTf)_3(bdmap)_2(H_2O)\cdot THF$ (**1**, $Gd^{III}Cu^{II}$); $[Gd(C_4H_7ON)_4(H_2O)_3][Fe(CN)_6]\cdot 2H_2O$ (**2**, $Gd^{III}Fe^{III}$); $[Gd(C_4H_7ON)_4(H_2O)_3][Cr(CN)_6]\cdot 2H_2O$ (**3**, $Gd^{III}Cr^{III}$). It is well-known that in the rare earth atom or its cation there is a strong orbital−spin interaction and both orbital and spin moments for electrons contribute to the molecular magnetic moment. However, in the case of Gd^{III}, the total orbital moment is equal to zero, so the magnetic moment comes only from the electronic spin. For these three compounds containing Gd^{III}, the problem of magnetic coupling becomes simpler.

The theoretical study of the magnetic behavior of binuclear complexes represents a great challenge to quantum chemical calculation due to the existence of a manifold of states separated by small energy differences. Up till now, the relation between the magnetic coupling mechanism and molecular structure was not clearly understood. An early qualitative approach aimed at considering the influence of molecular orbital factors in the nature of magnetic coupling was proposed by Hay, Thibeault, and Hoffmann.[7a] More precise theoretical estimates of the exchange coupling constants *J* can be obtained by using ab initio CI methods.[7b] However, the demanded computer capacity is highly challenging, so a certain degree of modelization for the molecule studied is required in ab initio methods, whose effects on the calculated parameters are unknown. Recently, some authors have explored a third way, consisting of the use of the density functional method (DFT) combined with the broken-symmetry (BS) approach proposed by Noodlemann.[8] This combined DFT−BS has been successfully applied to the study of the magnetic properties of iron−sulfur dimer and tetramer clusters and manganese−oxo dimer and tetramer compounds,[8]

* To whom correspondence should be addressed at Peking University. Fax: +86-10-62751708. E-mail: relab@pku.edu.cn.

10.1021/jp994093m CCC: $19.00
Published on Web 06/10/2000

as well as hydroxo-, alkoxo-,[1,9] and azido-bridged[2,3] Cu^{II} binuclear complexes. Fortunately, owing to the ability of the density functional method to handle large systems, the DFT−BS approach allows the calculation of the exchange coupling constants *J* for the complete structures of complex molecules with a good degree of accuracy. Also changes in substituents or counterions can be easily realized, thus allowing the evaluation of the effects of chemical substitutions on the magnetic behavior.

Spin density maps are helpful and informative in the description of the spin coupling mechanism between magnetic centers. Such maps may be experimentally obtained from the polarized neutron diffraction (PND)[4,5] and theoretically calculated by making use of quantum mechanical methods. The PND technique is quite complex and expensive, only available for limited compounds. Thus, we choose the computational method to make spin density maps for our target molecules. We apply herein the DFT−BS approach to study the magnetic coupling behavior for compounds **1**−**3**, giving the calculated exchange coupling constants *J* for complete structures and spin density maps for both high-spin (HS) and broken-symmetry (BS) states. It is worth pointing out that an understanding of the coupling mechanism is foreseen as a useful tool for the design of ferro- or antiferromagnetic interactions between magnetic centers in polynuclear systems. Particular emphasis in our work will be placed on analyses of the magnetic coupling mechanism.

Computational Details

The exchange coupling constants *J* for the title complexes have been evaluated by calculating the energy difference between the high-spin state (E_{HS}) and the broken-symmetry state (E_{BS}) (assuming the spin Hamiltonian is defined as $\hat{H} = -2J\hat{S}_1\cdot\hat{S}_2$), according to the following expression:[8a]

$$E_{HS} - E_{BS} = [-S_{max}(S_{max}+1) + \sum_{S}^{S_{max}} A_1(S)\cdot S(S+1)]J \quad (1)$$

where *S* corresponds to the spin states of the molecule studied and $A_1(S)$ stands for squares of Clebsch−Gordan coefficients. A positive value of the coupling constant *J* indicates a high-spin ground state with parallel spins (i.e. ferromagnetic character). For a negative value of *J*, the broken-symmetry state is lower in energy, with opposite spins on metal atoms giving rise to antiferromagnetic behavior. In the cases of **1**, $Gd^{III}Cu^{II}$, and **2**, $Gd^{III}Fe^{III}$, where $S_1 = {}^7/_2$ and $S_2 = {}^1/_2$, we obtained the expression as follows:

$$E_{HS} - E_{BS} = -7J \quad (2)$$

For the $Gd^{III}Cr^{III}$ complex, $S_1 = {}^7/_2$ and $S_2 = {}^3/_2$, the formula changes to

$$E_{HS} - E_{BS} = -21J \quad (3)$$

All calculations have been performed by using the Amsterdam density functional (ADF) package version 2.3.[10] The local density approximation (LDA) with local exchange and correlation potentials makes use of Vosko, Wilk, and Nusair's (VWN) correlation functionals.[11] Becke's nonlocal exchange correction[12] and Perdew's nonlocal correlation correction[13] are added in each SCF consistent cycle. For the complete structures of the molecules studied, we have used the IV basis sets in ADF, containing triple-ζ basis sets for all atoms and a polarization function from H to Ar atom. The frozen core (FC) approximation for the inner core electrons is used. The orbitals up to 5p for Gd and up to 3p for Cu, Cr, and Fe atoms are kept frozen. The numerical integration procedure applied for the calculations is the polyhedron method developed by Velde and co-workers.[14] Convergence is achieved once the maximum number of elements of the commutator of both the Fock matrix and the density matrix is smaller than 10^{-5} and the norm of the commutator is under 10^{-4} in absolute value. In this case, in fact, the convergence standard of the system energy is smaller than 10^{-6} eV, reaching a precision required for the evaluation of the *J* values. The spin density maps were obtained using program Cerius[2]. This program was developed by Molecular Simulations Inc.[15]

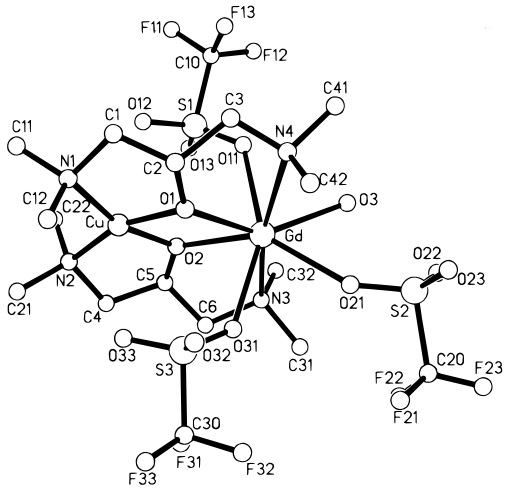

Figure 1. Molecular structure of complex $GdCu(OTf)_3(bdmap)_2(H_2O)\cdot THF$ (THF omitted).

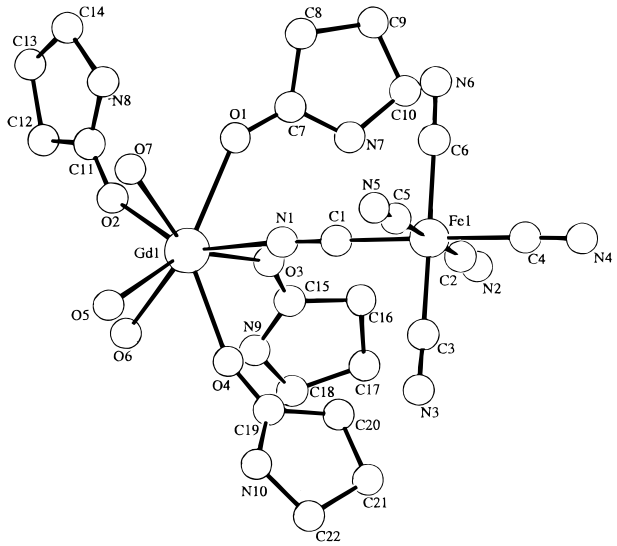

Figure 2. Molecular structure of complex $[Gd(C_4H_7ON)_4(H_2O)_3][Fe(CN)_6]\cdot 2H_2O$ (two crystal H_2O omitted).

The molecular structures for the title compounds **1**−**3** are taken from X-ray crystallography analyses[16,17] shown in Figures 1−3. The energies in both high-spin and broken-symmetry states are calculated for the complete molecules. Because the spin coupling is sensitive to any tiny change of the molecular structure, no simplification or optimization of the molecular structure is made in our calculations.

In $GdCu(OTf)_3(bdmap)_2(H_2O)\cdot THF$, Gd^{III} is 8-fold coordinated in an irregular manner by two alkoxo O atoms, three O atoms of OTf anions ($OTf = SO_3CF_3$), one O atom of water, and two N atoms of two bdmap, while Cu^{II} is 4-fold coordinated

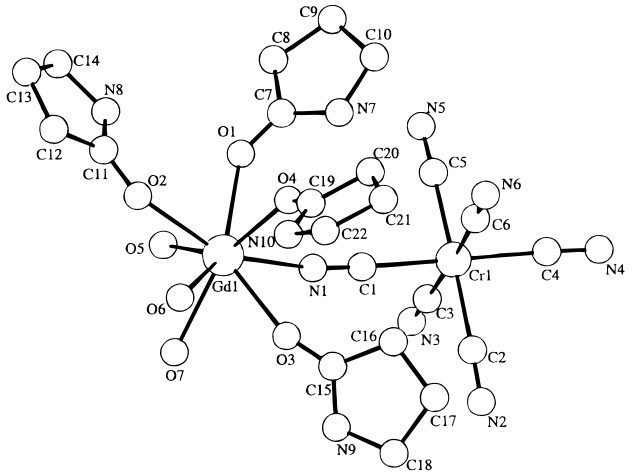

Figure 3. Molecular structure of complex $[Gd(C_4H_7ON)_4(H_2O)_3][Cr(CN)_6]\cdot 2H_2O$ (two crystal H_2O omitted).

TABLE 1: Magnetic Coupling Constants *J* (cm^{-1}) for the Compounds 1−3

	J	
compds	expt	DFT−BS
$GdCu(OTf)_3(bdmap)_2(H_2O)\cdot THF$	2.9(2)[16]	3.6
$[Gd(C_4H_7ON)_4(H_2O)_3][Fe(CN)_6]\cdot 2H_2O$	0.74(3)[17]	8.1
$[Gd(C_4H_7ON)_4(H_2O)_3][Cr(CN)_6]\cdot 2H_2O$	0.40(2)[17]	20.3

by two N and two O atoms of two bdmap, forming a slightly D_{2d}-distorted square (distances to the plane (Å): O1, 0.15; O2, −0.13; N1, −0.13; N2, 0.22 Å). Gd^{III} is linked with Cu^{II} through two alkoxo O atoms of bdmap (bdmap = 1,3-bis(dimethylamino)-2-propanol). The atoms Gd, Cu, O1, and O2 form a perfect plane. The bonding angles of Gd−O1−Cu, Gd−O2−Cu, O1−Gd−O2, and O1−Cu−O2 are 106.4, 104.7, 67.2, and 81.6°, respectively.

The compounds **2** and **3** have analogous molecular structures, with a bridging cyano ligand C1N1. For $[Gd(C_4H_7ON)_4(H_2O)_3][Fe(CN)_6]\cdot 2H_2O$ in Figure 2, the Fe atom is octahedrally coordinated by six cyano groups, with Fe−C distances in the range 1.932−1.949 Å, of which Fe1−C1 is 1.939 Å. The Gd atom is coordinated by one N atom from the bridging C1N1, four O atoms from 2-pyrrolidinone, and three water molecules. The coordination polyhedron of Gd is a square antiprism, with Gd1−N1 of 2.483 Å and Gd−O in the range of 2.344−2.421 Å. The angle of C1−N1−Gd1 is 162.1°. Similar to complex **2**, in the complex $[Gd(C_4H_7ON)_4(H_2O)_3][Cr(CN)_6]\cdot 2H_2O$, shown in Figure 3, the Cr^{III} atom is octahedrally coordinated by six cyano groups, with Cr−C distances in the range 2.066−2.092 Å. The distance of Cr1−Cl is 2.083 Å. The C−Cr−C angles are close to 90 or 180°. The Gd^{III} atom is coordinated by one N atom of C1N1, four O atoms from 2-pyrrolidinone, and three water molecules. The coordination polyhedron of Gd is a square antiprism; the N1, O2, O1w, and O5 define one plane of the square antiprism, and O1, O2w, O3, and O4, the other plane. The distance of Gd−N1 is 2.491 Å. The Gd−O distances are in the range 2.360−2.424 Å. The angle of C1−N1−Gd is 162.3°.

Results and Discussion

A. Magnetic Coupling Constant *J*. To examine the reliability of the DFT−BS approach in our discussion on spin coupling mechanism, we compare the calculated magnetic coupling constants *J* with experimental data, listed in Table 1. For $Gd^{III}Cu^{II}$,[16] $Gd^{III}Fe^{III}$,[17] and $Gd^{III}Cr^{III}$,[17] the signs of the *J* values are all positive, suggesting a ferromagnetic coupling between Gd^{III} and Cu^{II} (as well as Fe^{III} and Cr^{III}). The qualitative agreement between the calculated and experimental values of the coupling constants *J* is good, though there are some differences in absolute values. One must keep in mind that the *J* values are herein very small. In the case of $Gd^{III}Cu^{II}$ the calculated *J* value is 3.6 cm^{-1} close to experimental 2.9(2) cm^{-1}. In the cases of the other two molecules studied, we have the calculated value 8.1 cm^{-1} versus the experimental observation 0.74(3) cm^{-1} for $Gd^{III}Fe^{III}$ and the calculated 20.3 cm^{-1} versus the experimental 0.40(2) cm^{-1} for $Gd^{III}Cr^{III}$. Comparison between the calculated and experimental coupling constants *J* for the complete structures demonstrates that the DFT−BS approach is available for the compounds studied. The question we must now address is does the DFT−BS method provides a practical strategy for study on the magnetic coupling mechanism despite the existence of some uncertainty for the *J* value.

B. Spin Delocalization and Spin Polarization. In addition to the exchange coupling constants *J*, it is interesting to study the spin density distribution in these compounds. Some mechanisms have been proposed to explain the magnetic coupling behavior between two metal centers. Among them, the spin delocalization[18] and spin polarization mechanisms[19−22] succeed in dealing with the mononuclear and homobinuclear systems.[23] Here is a concise review on the main points of these two mechanisms by Cano et al.[23] The spin density distribution throughout a molecule of the coordination compound with paramagnetic centers results from the interplay of the two coupling mechanisms of the magnetic centers: spin delocalizaion and spin polarization. From the point of view of molecular orbital theory, the spin delocalizaion can be explained as a transfer of unpaired electron density from the metal atom to the ligand atoms, while the spin polarization results from the optimization of the electronic exchange and Coulomb terms and induces the spin distribution with alternating sign for the successive ligand atoms. Though the spin delocalization and spin polarization mechanisms are not specially proposed for heterobinuclear systems, we may also get some valuable hints for the systems studied by making use of these concepts.

C. Spin Density Distribution of $GdCu(OTf)_3(bdmap)_2(H_2O)\cdot THF$. The calculated spin density distributions for the high-spin (HS) and broken-symmetry states (BS) of the compound **1** are shown in Figure 4. The solid line depicts positive (α) spin density, and the dotted line indicates negative (β) spin density. From Figure 4a, we can see clearly that, in the HS state, the spin densities of Gd^{III} and Cu^{II} atoms are positive. The coordinating atoms around Cu^{II}, including N1, N2, O1, and O2, have positive spin densities too, demonstrating the spin delocalization from Cu^{II}. On the other hand, the spin densities of coordinating atoms around Gd^{III}, such as O3 and O4, are negative, suggesting a predominant effect of the spin polarization from Gd^{III}. It is evident that the bridging atoms, O1 and O2, are affected by both spin delocalization and spin polarization. Thus there exists a competition between the spin delocalization and spin polarization mechanisms. Apparently, spin delocalization of Cu^{II} gains the advantage here for the positive spin densities on the bridging atoms. In the BS state shown in Figure 4b, the spins on Cu^{II} have been flipped from α to β in the DFT−BS calculation. So the sign of the spin density on the bridging atoms changes with the sign of Cu^{II} simultaneously.

The spin populations in the high-spin and broken-symmetry states, obtained by DFT calculations on the basis of the Mulliken population analysis, are given in Table 3. The spin density on Gd^{III} is 7.0840 in the HS state and 7.0618 in the BS state,

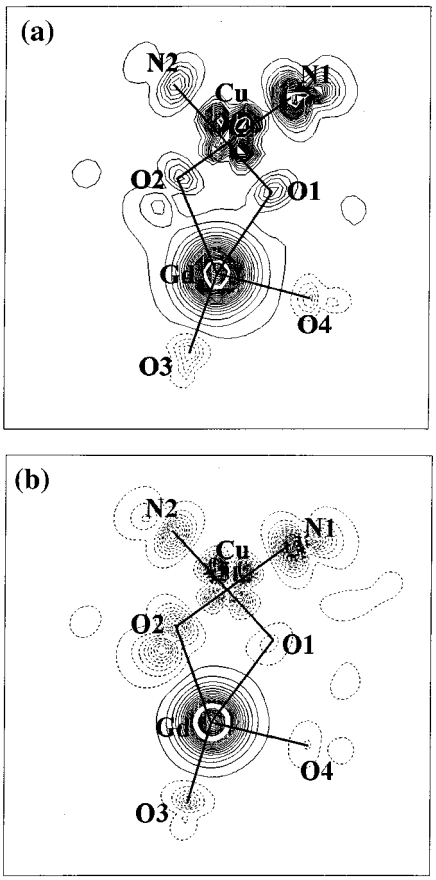

Figure 4. Spin density maps calculated for $GdCu(OTf)_3(bdmap)_2(H_2O)\cdot THF$ in projection on the N2−Cu−O2 plane: (a) for the high-spin (HS) state; (b) for the broken-symmetry (BS) state.

TABLE 2: Spin Densities Calculated for the High-Spin (HS) and Broken-Symmetry (BS) States of $GdCu(OTf)_3(bdmap)_2(H_2O)\cdot THF$

	$Gd^{III}Cu^{II}$			$Gd^{III}Cu^{II}$	
atom	HS	BS	atom	HS	BS
Gd	7.0840	7.0618	O21	−0.0139	−0.0138
O1	0.0959	−0.1559	O31	−0.0101	−0.0103
O2	0.0978	−0.1515	Cu	0.5380	−0.4854
O3	−0.0155	−0.0160	N1	0.0745	−0.0751
N3	−0.0106	−0.0118	N2	0.0873	−0.0878
N4	−0.0104	−0.0123	O12	0.0005	−0.0006
O11	−0.0124	−0.0129	O33	0.0004	−0.0007

which suggests seven 4f electrons are almost localized and not as active as the unpaired 3d electron on Cu^{II}. Thus Gd^{III} mainly displays its ionic nature and polarization effect. On the other hand, the spin density on Cu^{II} is 0.5380 (HS) and −0.4854 (BS) demonstrating an apparent spin delocalization effect. Compared with the greater spin densities on the bridging atoms, the other ligand atoms have very small spin densities. For instance, in the HS state the spin density on the bridging atom O1 is 0.0959, while for the peripheral atoms around Gd^{III} the spin densities are only 0.01 or so in absolute value. Due to the compensation of spin delocalization from Cu^{II} and spin polarization from Gd^{III}, the bridging atoms O1 and O2 have smaller spin densities (about 0.09) in the HS state than that in the BS state (about 0.15 in absolute value); in the latter the spin delocalization of Cu^{II} and spin polarization of Gd^{III} enhance complementally the spin densities on the bridging atoms.

D. Spin Density Distributions of $[Gd(C_4H_7ON)_4(H_2O)_3][Fe(CN)_6]\cdot 2H_2O$ and $[Gd(C_4H_7ON)_4(H_2O)_3][Cr(CN)_6]\cdot 2H_2O$. According to the spin density distribution in Figure 5, the main

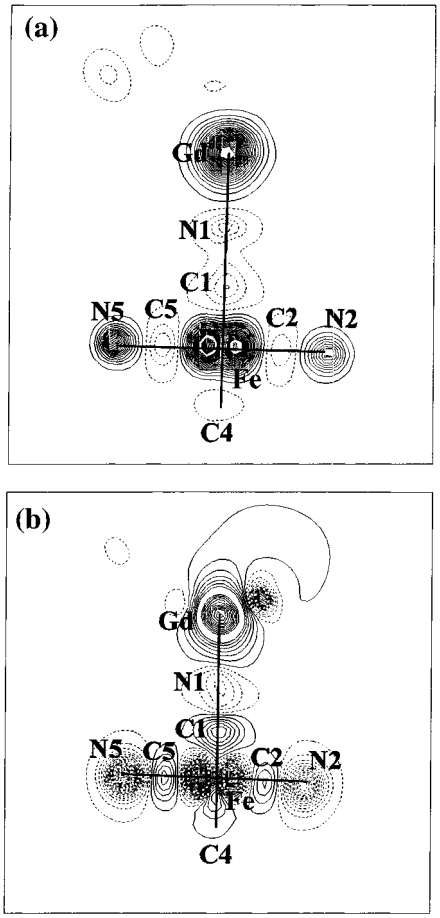

Figure 5. Spin density maps calculated for $[Gd(C_4H_7ON)_4(H_2O)_3][Fe(CN)_6]\cdot 2H_2O$ in projection on the C1−Fe−C5 plane: (a) for the high-spin (HS) state; (b) for the broken-symmetry (BS) state.

TABLE 3: Spin Densities Calculated for the High-Spin (HS) and Broken-Symmetry (BS) States of $[Gd(C_4H_7ON)_4(H_2O)_3][Fe(CN)_6]\cdot 2H_2O$ and $[Gd(C_4H_7ON)_4(H_2O)_3][Cr(CN)_6]\cdot 2H_2O$

	$Gd^{III}Fe^{III}$		$Gd^{III}Cr^{III}$	
atom	HS	BS	HS	BS
Gd	7.0084	7.2184	7.1639	7.0117
O1	−0.0151	−0.0166	−0.0159	−0.0147
O2	−0.0123	−0.0157	−0.0150	−0.0158
O3	−0.0134	−0.0162	−0.0142	−0.0137
O4	−0.0149	−0.0165	−0.0157	−0.0129
O5	−0.0114	−0.0117	−0.0131	−0.0126
O6	−0.0056	−0.0108	−0.0123	−0.0116
O7	−0.0120	−0.0133	−0.0119	−0.0111
Cr			2.9554	−3.0286
Fe	1.2727	−1.3396		
C1	−0.0332	0.0661	−0.0571	0.0655
C2	−0.0562	0.0367	−0.1222	0.1229
C3	−0.0492	0.0528	−0.1256	0.1271
C4	−0.0462	0.0652	−0.1406	0.1439
C5	−0.0557	0.0430	−0.1225	0.1230
C6	−0.0510	0.0543	−0.1048	0.1048
N1	−0.0177	−0.0634	0.0289	−0.0770
N2	0.0632	−0.0130	0.1003	−0.1002
N3	0.0540	−0.0650	0.0921	−0.1008
N4	0.0582	−0.1240	0.0995	−0.1139
N5	0.0935	−0.0346	0.0995	−0.0989
N6	0.0548	−0.0702	0.0784	0.0815

finding may be summed up as follows. In the HS state of $Gd^{III}Fe^{III}$, large positive densities are found on the Fe^{III} and Gd^{III} atoms, respectively. The spin densities in the first coordination shell of the Fe^{III} and Gd^{III} atoms are negative, arising from spin

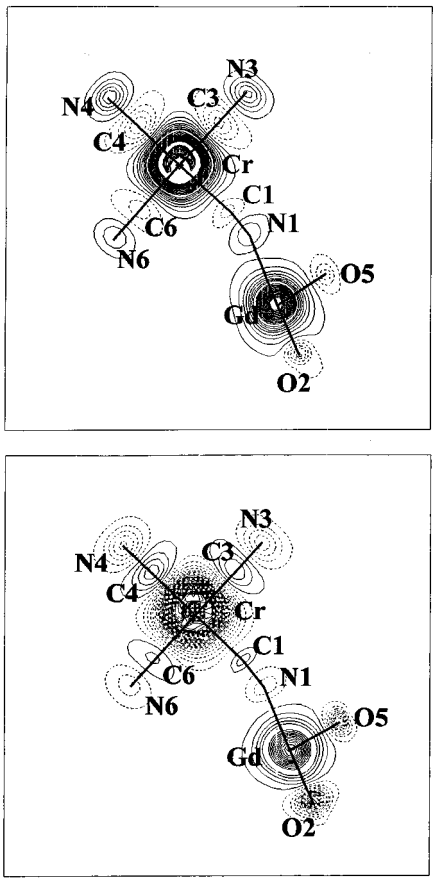

Figure 6. Spin density maps calculated for $[Gd(C_4H_7ON)_4(H_2O)_3][Cr(CN)_6]\cdot 2H_2O$ in projection on the C3−Cr−C4 plane: (a) for the high-spin (HS) state; (b) for the broken-symmetry (BS) state.

polarization of Fe^{III} and Gd^{III}. In Table 3, the spin populations of six carbon atoms around Fe^{III} in HS vary from −0.0332 to −0.0562, which are less in absolute value than those of Cu^{II} in $Gd^{III}Cu^{II}$. The spin densities of coordinating atoms around Cu^{II}, such as N1, N2, O1, and O2, range from 0.0745 to 0.0978. Furthermore, it is evident that the spin density is not equally polarized for the six coordinating carbon atoms around Fe^{III}. Apparently, the spin densities at the five terminal carbon atoms (C2, C3, C4, C5, C6) (cf. Table 3), which are −0.0562, −0.0492, −0.0462, −0.0557, and −0.0510, respectively, predominate over the spin density at the bridging C1 (−0.0332). Because the polarization effect propagates with the alternate spin sign away from the paramagnetic center, this phenomenon clearly associates with the compensation nature of the spin polarization from Gd^{III}. According to the spin polarization effect of Gd^{III}, the bridging C1 atom should have a positive spin density. However, the calculated spin density on C1 is −0.0332. It is shown that on the bridging C1 the spin polarization from Fe^{III} predominates over that of Gd^{III}. In the case of the bridging N1 atom, vice versa, the spin polarization from Gd^{III} is over that from Fe^{III}. In the BS state for $Gd^{III}Fe^{III}$ the spin polarization effects from both Fe^{III} and Gd^{III} on the bridging ligand C1N1 enhance the spin densities on C1 and N1 because the polarization effects are complementary.

For the compound $Gd^{III}Cr^{III}$ in the HS state, the spin densities of ligand atoms around Cr^{III} and Gd^{III} are also negative, showing the spin polarization mechanism of two magnetic centers (cf. Figure 6). For the bridging ligand C1N1, the spin polarization from the Cr^{III} atom leads to a negative spin on C1 and a positive spin on N1; in contrast, the spin polarization of Gd^{III} should result in a positive spin on C1 and a negative spin on N1. However, the counteracting effect of the opposite polarization leads to a low spin density on the bridging ligand C1N1, compared with the other five CN ligands. In fact, the spin densities on C1 and N1 are −0.0571 and 0.0289, respectively, while spin densities on other C and N are relatively greater, such as C2 (−0.1222) and N2 (0.1003) (cf. Table 3). In contrast to $Gd^{III}Fe^{III}$ in HS with the negative spin density on the N1 atom, the spin density on the N1 atom in $Gd^{III}Cr^{III}$ is positive, showing a predominant effect of spin polarization from Cr^{III}. Thus Cr^{III} in $Gd^{III}Cr^{III}$ has the stronger spin polarization effect compared to Fe^{III} in $Gd^{III}Fe^{III}$.

Conclusions

On the whole, we can see that the unpaired 4f electrons on Gd^{III} always demonstrate a polarization effect, while the unpaired 3d electrons of Cu^{II}, Cr^{III}, and Fe^{III} play a versatile role in the magnetic coupling mechanism. For **1**, the spin delocalization from Cu^{II} and spin polarization from Gd^{III} determine that the HS state is its ground state, and the coupling between Cu^{II} and Gd^{III} is ferromagnetic with the calculated J of 3.6 cm^{-1}. For **2**, the spin polarization from Fe^{III} and Gd^{III} makes HS lower in energy than BS, so its coupling is ferromagnetic. For **3**, both Cr^{III} and Gd^{III} demonstrate spin polarization effects, in which Cr^{III} has the stronger influence on the bridging atoms than Fe^{III}. The counteraction between the opposite spin polarizations from Gd^{III} and Fe^{III} or Cr^{III} makes the spin densities on the bridging atoms lower and leads to the ferromagnetic coupling between Gd^{III} and Fe^{III} or Cr^{III}, with the calculated J of 8.1 cm^{-1} for **2** and J of 20.3 cm^{-1} for **3**. Thus we could come to the following conclusion: to decide the coupling nature of ferro- or antiferromagnetism, the spin delocalization and spin polarization mechanisms as well as their counteractive or complementary effects must be considered together.

Acknowledgment. This project is supported by the National Nature Science Foundation of China (Grants 29831010, 20023005) and State Key Project of Fundamental Research of China (Grant G 1998061306). We sincerely thank Prof. Song Gao for providing us experimental data for $GdCu(OTf)_3(bdmap)_2(H_2O)\cdot THF$ and thank Dr. Xianru Sun for the synthesis and measurement of the magnetic properties of two wonderful compounds: $[Gd(C_4H_7ON)_4(H_2O)_3][Cr(CN)_6]\cdot 2H_2O$ and $[Gd(C_4H_7ON)_4(H_2O)_3][Fe(CN)_6]\cdot 2H_2O$. The authors thank Dr. Noodleman (The Scripps Research Institute) for helpful discussions and the introduction on the broken-symmetry approach.

References and Notes

(1) Ruiz, E.; Alemany, P.; Alvarez, S.; Cano, J. *J. Am. Chem. Soc.* **1997**, *119*, 1297.

(2) Ruiz, E.; Cano, J.; Alvarez, S.; Alemany, P. *J. Am. Chem. Soc.* **1998**, *120*, 11122.

(3) Adamo, C.; Barone, V.; Bencini, A.; Totti, F.; Ciofini, I. *Inorg. Chem.* **1999**, *38*, 1996.

(4) Barone, V.; Gillon, B.; Plantevin, O.; Cousson, A.; Mathonière, C.; Kahn, O.; Grand, A.; Öhrströnm, L.; Delley, B. *J. Am. Chem. Soc.* **1996**, *118*, 11822.

(5) Aebersold, M. A.; Gillon, B.; Plantevin, O.; Pardi; L.; Kahn, O.; Bergerat. P.; von Seggern, I.; Tuczek, F.; Öhrströnm, L.; Grand, A.; Lelièvre-Berna, E. *J. Am. Chem. Soc.* **1998**, *120*, 5238.

(6) Costes, J.-P.; Dahan, F.; Dupuis, A.; Laurent, J.-P. *Inorg. Chem.* **1997**, *36*, 3429.

(7) (a) Hay, P. J.; Thibeault, J. C.; Hoffmann. R. *J. Am. chem. Soc.* **1975**, *97*, 4884. (b) Castell, O.; Caballol, R.; Garcia, V. M.; Handrick, K. *Inorg. Chem.* **1996**, *35*, 1609. Miralles, J.; Castell, O.; Caballol, R. *Chem. Phys.* **1994**, *179*, 337. Nishino, M.; Yamanaka, S.; Yoshioka, Y.; Yamaguchi, K. *J. Phys. Chem.* **1997**, *101*, 705.

(8) (a) Noodleman, L. *J. Chem. Phys.* **1981**, *74*, 5737. (b) Noodleman, L.; Baerends, E. J. *J. Am. Chem. Soc.* **1984**, *106*, 2316. (c) Noodleman, L.; Case, D. A. *Adv. Inorg. Chem.* **1992**, *38*, 423. (d) Li, J.; Noodleman, L.; Case, D. A. In *Inorganic Electronic Structure and Spectroscopy*; Solomon, E. I., Lever, A. B. P., Eds.; New York: Wiley 1999; Vol. I, pp 661−724.

(9) Ruiz, E.; Alemany, P.; Alvarez, S.; Cano, J. *Inorg. Chem.* **1997**, *36*, 3683.

(10) Amsterdam Density Functional (ADF), version 2.3; Scientific Computing and Modelling, Theoretical Chemistry, Virje Universiteit: Amsterdam, 1997.

(11) Vosko, S. H.; Wilk, L.; Nusair, M. *Can. J. Phys*. **1980**, *58*, 1200.

(12) Becke, A. D. *Phys. Rev. A* **1988**, *38*, 3098.

(13) Perdew, J. P. *Phys. Rev. B* **1986**, *33*, 8822.

(14) (a) Boerrigter, P. M.; Velde, G. T.; Baerends, E. J. *Int. J. Quantum Chem.* **1988**, *33*, 87. (b) Velde, G. T.; Baelends, E. J. *J. Comput. Phys.* **1992**, *99*, 84.

(15) Molecular Simulations Inc., San Diego, CA.

(16) Gao, S.; Borgmeier, O.; Lueken, H. *The Third International Conference of f Elements Abstract Book*; Porcher, P., Hölsä, J., Eds.; Paris, Sep 1997.

(17) Sun, X. R. Ph.D. Thesis, Peking University, Beijing, 1999.

(18) Kahn, O. *Molecular Magnetism*; VCH: New York, 1993.

(19) McConnell, H. M. *J. Chem. Phys.* **1963**, *39*, 1910.

(20) Izuoka, A.; Murata, S.; Sugawara, T.; Iwamura, H.*J. Am. Chem. Soc.* **1987**, *109*, 2631.

(21) Charlot, M.-F.; Kahn, O.; Chaillet, M.; Larrieu, C. *J. Am. Chem. Soc.* **1986**, *108*, 2574.

(22) Albright, T. A.; Burdett, J. K.; Whangbo, M.-H. *Orbital Interactions in Chemistry*; Wiley: New York, 1985.

(23) Cano, J.; Ruiz, E.; Alvarez, S.; Verdaguer, M. *Comments Inorg. Chem*. **1998**, *20*, 27.